

RESEARCH ARTICLE

Open Access



Analyses of the peripheral immunome following multiple administrations of avelumab, a human IgG1 anti-PD-L1 monoclonal antibody

Renee N. Donahue^{1†}, Lauren M. Lepone^{1†}, Italia Grenga¹, Caroline Jochems¹, Massimo Fantini¹, Ravi A. Madan², Christopher R. Heery¹, James L. Gulley^{2†} and Jeffrey Schlom^{1*†} 

Abstract

Background: Multiple anti-PD-L1/PD-1 checkpoint monoclonal antibodies (MAb) have shown clear evidence of clinical benefit. All except one have been designed or engineered to omit the possibility to mediate antibody-dependent cell-mediated cytotoxicity (ADCC) as a second potential mode of anti-tumor activity; the reason for this is the concern of lysis of PD-L1 positive immune cells. Avelumab is a fully human IgG1 MAb which has been shown in prior in vitro studies to mediate ADCC versus a range of human tumor cells, and clinical studies have demonstrated anti-tumor activity versus a range of human cancers. This study was designed to investigate the effect on immune cell subsets in the peripheral blood of cancer patients prior to and following multiple administrations of avelumab.

Methods: One hundred twenty-three distinct immune cell subsets in the peripheral blood of cancer patients ($n = 28$) in a phase I trial were analyzed by flow cytometry prior to and following one, three, and nine cycles of avelumab. Changes in soluble (s) CD27 and sCD40L in plasma were also evaluated. In vitro studies were also performed to determine if avelumab would mediate ADCC of PBMC.

Results: No statistically significant changes in any of the 123 immune cell subsets analyzed were observed at any dose level, or number of doses, of avelumab. Increases in the ratio of sCD27:sCD40L were observed, suggesting potential immune activation. Controlled in vitro studies also showed lysis of tumor cells by avelumab versus no lysis of PBMC from five donors.

Conclusions: These studies demonstrate the lack of any significant effect on multiple immune cell subsets, even those expressing PD-L1, following multiple cycles of avelumab. These results complement prior studies showing anti-tumor effects of avelumab and comparable levels of adverse events with avelumab versus other anti-PD-1/PD-L1 MAbs. These studies provide the rationale to further exploit the potential ADCC mechanism of action of avelumab as well as other human IgG1 checkpoint inhibitors.

Trial registration: ClinicalTrials.gov identifier: NCT01772004 (first received: 1/14/13; start date: January 2013) and NCT00001846 (first received date: 11/3/99; start date: August 1999).

Keywords: Avelumab, Anti-PD-L1, Checkpoint inhibitor, Immunotherapy, Peripheral immunome, Immune subsets, ADCC, Antibody-dependent cell-mediated cytotoxicity

* Correspondence: js141c@nih.gov

†Equal contributors

RND and LML contributed equally in terms of conducting the majority of experiments and responsibility for the work, while JLG and JS, the senior authors, contributed equally in terms of overview of the project

¹Laboratory of Tumor Immunology and Biology, Center for Cancer Research, National Cancer Institute, National Institutes of Health, 10 Center Drive, Room 8B09, Bethesda, MD, USA

Full list of author information is available at the end of the article



Background

Immune checkpoint inhibition employing monoclonal antibodies (MAbs) directed against programmed cell death protein 1 (PD-1) or programmed cell death protein-1 ligand (PD-L1) has been a major advance in the management of selected patients in several tumor types and stages (see [1, 2] for recent reviews). The general concept is that the interaction of PD-1 on immune cells with PD-L1 on tumor cells can lead to immune cell anergy and thus the lack of anti-tumor activity; the use of either anti-PD-1 or PD-L1 MAbs is designed to block this interaction leading to tumor cell lysis. The use of a human anti-PD-L1 MAb of the IgG1 isotype could potentially add another mode of anti-tumor activity. Human IgG1 MAbs have been shown to be capable of mediating antibody-dependent cell-mediated cytotoxicity (ADCC) via the interaction of the IgG1 Fc region with its ligand on human natural killer (NK) cells. One caution in the use of this approach is that several human immune cell populations also express PD-L1, and could thus potentially also be susceptible to ADCC-mediated lysis. It is for this reason that, with one exception, all of the anti-PD-L1 MAbs in clinical studies to date were constructed as either an IgG4 isotype that cannot mediate ADCC, or an IgG1 MAb engineered to be devoid of ADCC activity; the one exception is the development of the human IgG1 anti-PD-L1 MAb avelumab (MSB0010718C). We have previously shown that avelumab can mediate ADCC in vitro using as targets a range of human tumor cell lines that express PD-L1, and that this lysis can be blocked using an anti-CD16 antibody to inhibit the interaction of CD16 on NK cells with the IgG1 Fc receptor on avelumab [3–5]. We have also shown that avelumab can mediate tumor lysis in vivo using a murine tumor model [6]. A recent study also showed that the addition of avelumab to an in vitro assay leads to enhanced antigen-specific T-cell activation [7]. A Phase I dose escalation trial (NCT01772004) and use of avelumab in multiple expansion cohorts have shown evidence of clinical benefit of avelumab in patients with thymoma, mesothelioma, non-small cell lung cancer (NSCLC), ovarian, gastric and urothelial cancer, among others [8–13]. A recent phase II study [14] also demonstrated clinical activity of avelumab in Merkel cell carcinoma. In the dose escalation trial, there were no dose-limiting toxicities (DLT) in dose levels 1, 2, and 3 (1, 3, and 10 mg/kg) and one DLT on dose level 4 (20 mg/kg) concurrent with an anti-tumor response [[11]; Heery, et al. First-in-human phase 1 dose-escalation trial of avelumab. *Lancet Oncol.*, In press]. At the time of writing, multiple Phase III trials of avelumab are ongoing in patients with a range of tumor types and stages.

As mentioned above, one of the concerns in the use of an IgG1 anti-PD-L1 MAb is the potential effect on PD-

L1 expressing immune cells. We have recently described a methodology in which 123 different immune cell subsets can be analyzed by flow cytometry using one tube of blood (approximately 10^7 peripheral blood mononuclear cells (PBMC)). We have previously reported the relative distributions of these 123 classic and refined subsets in healthy donors vs. metastatic cancer patients [15]. In this study, we interrogated the effect of administration of different doses of avelumab on multiple peripheral immune cell subsets; the 123 immune cell subsets were analyzed prior to and following one, three and nine cycles of avelumab every 2 weeks. The effect of avelumab administration on changes in soluble CD27 (sCD27) and soluble CD40 ligand (sCD40L) in plasma was also evaluated. In controlled studies, the ability of avelumab to mediate ADCC of tumor cells vs. peripheral immune cells was conducted using NK cells as effectors from five different healthy donors and three cancer patients. Potential strategies to exploit the ADCC potential of avelumab are also discussed.

Methods

Cancer patients and healthy donors

Flow cytometry analysis was performed on PBMC of cancer patients who were enrolled in a first-in-human, open-label, dose-escalation and expansion Phase 1 clinical trial (NCT01772004). The National Cancer Institute Institutional Review Board approved the trial procedures and informed consent was obtained in accordance with the Declaration of Helsinki. Metastatic cancer patients with solid tumors were treated with 1, 3, 10 or 20 mg/kg of avelumab every 2 weeks [Heery, et al. First-in-human phase 1 dose-escalation trial of avelumab. *Lancet Oncol.*, In press]. Based on PBMC availability, the flow cytometry analysis included 28 patients with 12 different types of solid tumors: adrenocortical ($n = 2$), breast ($n = 3$), chordoma ($n = 1$), gastrointestinal (GI) ($n = 7$), lung ($n = 1$), mesothelioma ($n = 3$), neuroendocrine ($n = 1$), ovarian ($n = 1$), pancreatic ($n = 4$), prostate ($n = 1$), renal cell ($n = 3$) and spindle cell ($n = 1$) cancer. Patients received 1 or 3 mg/kg ($n = 11$), 10 mg/kg ($n = 8$), or 20 mg/kg ($n = 9$) of avelumab. Based on plasma availability, the soluble factor analysis included 39 patients receiving 1 or 3 mg/kg ($n = 15$), 10 mg/kg ($n = 13$), or 20 mg/kg ($n = 11$) of avelumab. PBMC for in vitro ADCC assays were obtained from five healthy donors from the NIH Clinical Center Blood Bank (NCT00001846) and three NSCLC patients enrolled in a previously described trial before the initiation of therapy [16]. PBMC for the antibody competition assay were obtained from a patient with metastatic castration resistant prostate cancer (mCRPC) enrolled in a previously described trial before the initiation of therapy [17].

Multicolor flow cytometry

Multicolor flow cytometry was performed on frozen PBMC as previously described [15]. One vial of PBMC containing 10^7 cells was thawed per cancer patient prior to therapy ($n = 28$) and 2 weeks after patients were administered the first cycle (PBMC tested on ~ day 15, $n = 19$), third cycle (PBMC tested on ~ day 43, $n = 14$), and ninth cycle (PBMC tested on ~ day 127, $n = 16$) of avelumab. PBMC were counted and assessed for cell viability with trypan blue exclusion. Median cell viability was 92% (89–95% interquartile range), and less than 5% of PBMC samples assayed from the trial (4/81) had

viabilities <80%. Samples with viability <80% were annotated in the analysis to ensure that low viability did not impact the ability to detect PD-L1. PBMC were stained with five different antibody panels (Additional file 1: Table S1). These panels identified markers involved in PD-1 signaling (panel 1), CD4⁺ and CD8⁺ T cells, and B cells (panel 2), regulatory T cells (Tregs) (panel 3), NK cells, NK-T cells, conventional dendritic cells (cDC) and plasmacytoid DC (pDC) (panel 4), and myeloid derived suppressor cells (MDSC) (panel 5). A total of 123 peripheral immune cell subsets were analyzed (Table 1 and Additional file 1: Table S2), which included nine

Table 1 Complete list of 123 peripheral immune cell subsets analyzed by flow cytometry

1. Total CD4 ⁺ T cells	• Total central memory (CCR7 ⁺ CD45RA ⁻) CD8	• Total immature (CD16 ⁻ CD56 ^{br}) NK
• PD-L1 ⁺ CD4	◦ PD-L1 ⁺ CM CD8	◦ PD-L1 ⁺ immature NK
• PD-1 ⁺ CD4	◦ PD-1 ⁺ CM CD8	◦ PD-1 ⁺ immature NK
• EOMES ⁺ CD4	◦ CTLA-4 ⁺ CM CD8	◦ Tim-3 ⁺ immature NK
• TCR ⁺ CD4	◦ Tim-3 ⁺ CM CD8	• Total unconventional (CD16 ⁻ CD56 ^{dim}) NK
• Tbet ⁺ CD4	• Total effector memory (CCR7 ⁻ CD45RA ⁺) CD8	◦ PD-L1 ⁺ unconventional NK
• BATF ⁺ CD4	◦ PD-L1 ⁺ EM CD8	◦ PD-1 ⁺ unconventional NK
• CTLA-4 ⁺ CD4	◦ PD-1 ⁺ EM CD8	◦ Tim-3 ⁺ unconventional NK
• Tim-3 ⁺ CD4	◦ CTLA-4 ⁺ EM CD8	6. Total NK-T
• ICOS ⁺ CD4	◦ Tim-3 ⁺ EM CD8	• PD-L1 ⁺ NK-T
◦ PD-L1 ⁺ ICOS ⁺ CD4	• Total EMRA (CCR7 ⁻ CD45RA ⁺) CD8	• PD-1 ⁺ NK-T
◦ PD-1 ⁺ ICOS ⁺ CD4	◦ PD-L1 ⁺ EMRA CD8	• Tim-3 ⁺ NK-T
• Total naïve (CCR7 ⁺ CD45RA ⁺) CD4	◦ PD-1 ⁺ EMRA CD8	7. Total cDC
◦ PD-L1 ⁺ naïve CD4	◦ CTLA-4 ⁺ EMRA CD8	• PD-L1 ⁺ cDC
◦ PD-1 ⁺ naïve CD4	◦ Tim-3 ⁺ EMRA CD8	• PD-1 ⁺ cDC
◦ CTLA-4 ⁺ naïve CD4	3. Total Tregs	• CD83 ⁺ cDC
◦ Tim-3 ⁺ naïve CD4	• PD-L1 ⁺ Tregs	• Tim-3 ⁺ cDC
• Total central memory (CCR7 ⁺ CD45RA ⁻) CD4	• PD-1 ⁺ Tregs	8. Total pDC
◦ PD-L1 ⁺ CM CD4	• CTLA-4 ⁺ Tregs	• PD-L1 ⁺ pDC
◦ PD-1 ⁺ CM CD4	• ICOS ⁺ Tregs	• PD-1 ⁺ pDC
◦ CTLA-4 ⁺ CM CD4	• CD45RA ⁺ Tregs	• CD83 ⁺ pDC
◦ Tim-3 ⁺ CM CD4	• CD49d ⁺ Tregs	• Tim-3 ⁺ pDC
• Total effector memory (CCR7 ⁻ CD45RA ⁺) CD4	4. Total B cells	9. Total MDSC
◦ PD-L1 ⁺ EM CD4	• PD-L1 ⁺ B cells	• PD-L1 ⁺ MDSC
◦ PD-1 ⁺ EM CD4	• PD-1 ⁺ B cells	• PD-1 ⁺ MDSC
◦ CTLA-4 ⁺ EM CD4	• CTLA-4 ⁺ B cells	• CD16 ⁺ MDSC
◦ Tim-3 ⁺ EM CD4	• Tim-3 ⁺ B cells	• Total monocytic (CD14 ⁺ CD15 ⁻) MDSC
• Total EMRA (CCR7 ⁻ CD45RA ⁺) CD4	5. Total NK	◦ PD-L1 ⁺ mMDSC
◦ PD-L1 ⁺ EMRA CD4	• PD-L1 ⁺ NK	◦ PD-1 ⁺ mMDSC
◦ PD-1 ⁺ EMRA CD4	• PD-1 ⁺ NK	◦ CD16 ⁺ mMDSC
◦ CTLA-4 ⁺ EMRA CD4	• Tim-3 ⁺ NK	• Total granulocytic (CD14 ⁻ CD15 ⁺) MDSC
◦ Tim-3 ⁺ EMRA CD4	• Total mature (CD16 ⁺ CD56 ^{dim}) NK	◦ PD-L1 ⁺ gMDSC
2. Total CD8 ⁺ T cells	◦ PD-L1 ⁺ mature NK	◦ PD-1 ⁺ gMDSC
• PD-L1 ⁺ CD8	◦ PD-1 ⁺ mature NK	◦ CD16 ⁺ gMDSC
• PD-1 ⁺ CD8	◦ Tim-3 ⁺ mature NK	• Total lineage negative (CD14 ⁻ CD15 ⁻) MDSC
• EOMES ⁺ CD8	• Total functional intermediate (CD16 ⁺ CD56 ^{br}) NK	◦ PD-L1 ⁺ lin neg MDSC
• TCR ⁺ CD8	◦ PD-L1 ⁺ functional intermediate NK	◦ PD-1 ⁺ lin neg MDSC
• Tbet ⁺ CD8	◦ PD-1 ⁺ functional intermediate NK	◦ CD16 ⁺ lin neg MDSC
• BATF ⁺ CD8	◦ Tim-3 ⁺ functional intermediate NK	
• CTLA-4 ⁺ CD8		
• Tim-3 ⁺ CD8		
• Total naïve (CCR7 ⁺ CD45RA ⁺) CD8		
◦ PD-L1 ⁺ naïve CD8		
◦ PD-1 ⁺ naïve CD8		
◦ CTLA-4 ⁺ naïve CD8		
◦ Tim-3 ⁺ naïve CD8		

Nine classic subsets were identified as well as 114 refined subsets relating to maturation and function within the classic subsets (Lepone et al., ref. [15])
 BATF basic leucine zipper transcription factor ATF-like, cDC conventional dendritic cells, CM central memory, CTLA-4 cytotoxic T lymphocyte-associated protein-4, EM effector memory, EMRA terminally differentiated effector memory, EOMES eomesodermin, gMDSC granulocytic MDSC, ICOS inducible T cell co-stimulator, lin neg MDSC lineage negative MDSC, MDSC myeloid derived suppressor cell, mMDSC monocytic MDSC, NK natural killer, pDC plasmacytoid DC, PD-1 programmed cell death protein 1, PD-L1 programmed cell death ligand-1, Tbet T box expressed in T cells, TCR T cell receptor, Tim-3 T cell immunoglobulin and mucin domain-3, Tregs regulatory T cells

classic immune cell subsets, 25 PD-L1⁺ subsets, and 89 refined subsets related to maturation and function. Following staining, samples were acquired on a BD LSRII cytometer (BD Biosciences, San Jose, CA) equipped with four lasers (UV, violet, blue, and red). The cytometer is serviced by BD technicians under a service contract, and is calibrated daily before use with cytometer setup and tracking beads to ensure quality performance. The laser configuration and filter sets are shown in Additional file 2: Figure S1. Voltages were adjusted to allow both negative and positive signals to be visualized and to minimize spectral overlap between channels. FCS files were exported and analyzed using FlowJo v9.7 for Macintosh (Treestar, Ashland, OR) using the outlined gating strategy (Fig. 1), with non-viable cells excluded and negative gates set based on fluorescence minus one controls. Compensation was performed in FlowJo using beads (BD Biosciences) that were single stained with each of the antibodies in the 5 panels. The frequency of all subsets was calculated as a percentage of PBMC to help eliminate the bias that could occur in the smaller populations with fluctuations in leukocyte subpopulations. The methodology used to analyze the flow cytometry data in the current study is identical to that of Lepone et al. [15].

Measurement of soluble factors in plasma

Plasma levels of sCD27 and sCD40L were determined using human sCD27 and sCD40L Instant ELISA kits (eBioscience, San Diego, CA). One vial of frozen plasma per cancer patient was assayed prior to therapy and following one cycle (~day 15, $n = 39$) and three cycles (~day 43, $n = 33$) of avelumab.

In vitro ADCC assay

NK effectors were isolated from PBMC using the Human NK Cell Isolation (negative selection) Kit (Miltenyi Biotech, San Diego CA) following the manufacturer's protocol, resulting in >90% purity. NK cells were allowed to rest overnight in RPMI 1640 medium (Corning Cellgro, Manassas, VA) supplemented with 10% human AB serum (Omega Scientific, Tarzana, CA), 100 U/mL penicillin, 100 µg/mL streptomycin and 2 mM L-glutamine (Corning Cellgro, Corning, NY).

Human lung NCI-H441 [H441] (ATCC[®] HTB-174[™]) and NCI-H460 [H460] (ATCC[®] HTB-177[™]) carcinoma cells as well as PBMC from healthy donors and cancer patients were used as targets with purified NK cells as effectors in the presence of avelumab or isotype control antibody at a concentration of 1 ng/mL. Prior to use as targets in the ADCC assay, PBMC from cancer patients were sorted to enrich for PD-L1⁺ and PD-L1⁻ cells; PBMC were rested overnight, stained with PD-L1-PE-Cy7 (clone MIH-1, BD Biosciences) followed by Anti-Cy7

microbeads (Miltenyi Biotech) and PD-L1⁺ and PD-L1⁻ fractions isolated by magnetic selection. To determine the ADCC activity, a 4-h ¹¹¹In-release assay was performed, as previously described [3]. Effector cell-to-target cell (E:T) were used at ratios of 25:1, 12.5:1 and 6.25:1 for assays with healthy donor NK, and 25:1 for experiments with cancer patient NK. Spontaneous release was determined by incubation of target cells with medium alone, and complete lysis by incubation with 0.05% Triton X-100. Specific ADCC lysis was determined using the following equation: percent lysis = (experimental - spontaneous)/(complete - spontaneous) x 100.

Antibody competition assay

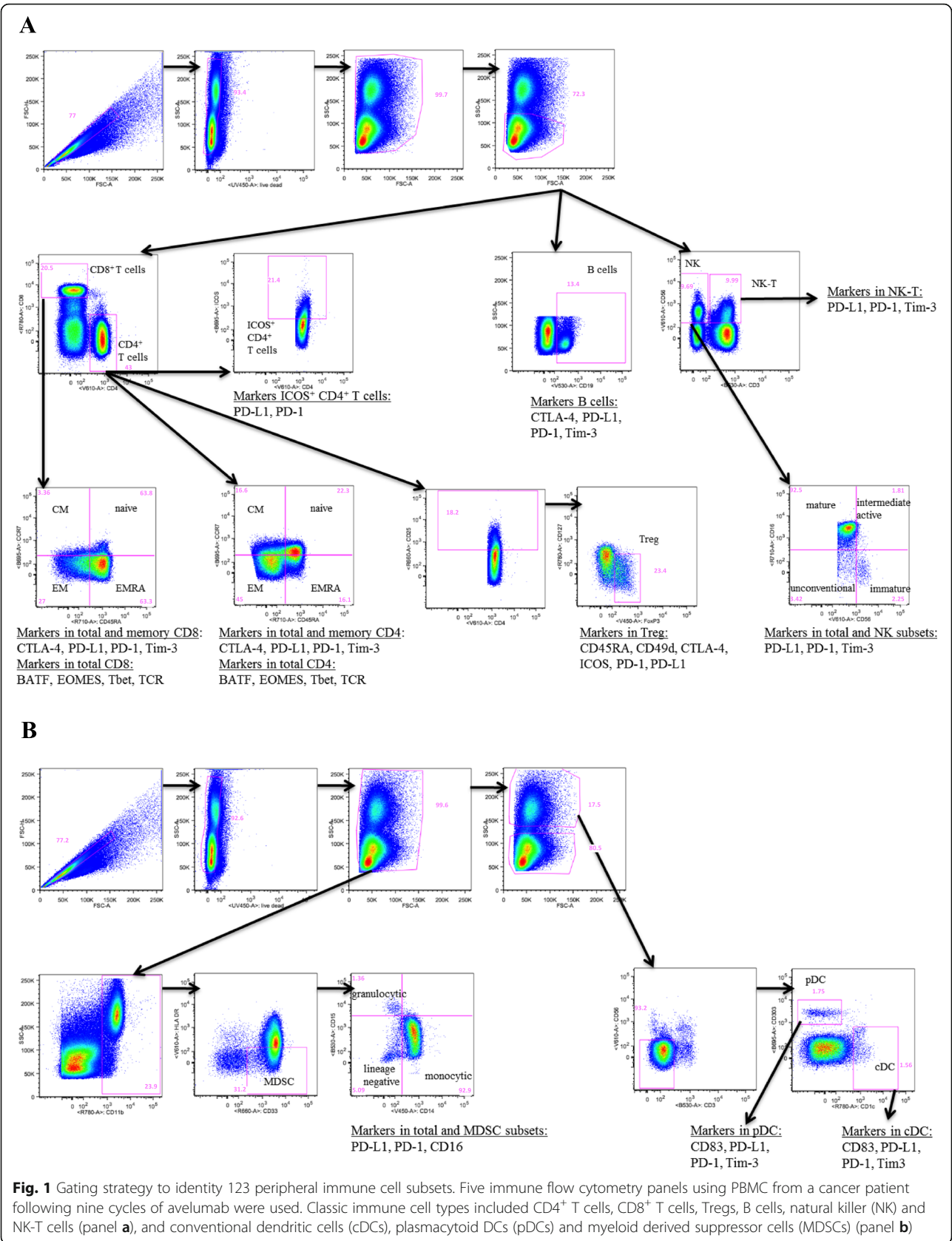
PBMC from a cancer patient with mCRPC were rested for 48 h and then pre-incubated for 30 min with avelumab or IgG1 isotype control at 0.2, 2, and 20 µg/mL, washed and then stained with multiparametric flow cytometry, as described above, to detect PD-L1 (with the MIH-1 clone) within the various immune cell types. PBMC that were not pre-incubated with avelumab or the isotype control also served as controls. The frequency of PD-L1 within each of the classic immune cell types was determined both as a percentage of parent and total PBMC.

FcγRIIIa (CD16) genotyping

To examine the polymorphism of CD16 (valine (V) versus phenylalanine (F) substitution at amino acid position 158), DNA was extracted from PBMC of healthy donors and cancer patients receiving avelumab using the QIAamp DNA Blood Mini kit (Qiagen, Valencia, CA) and stored at -80 °C until use. The FcγRIIIa (CD16) genotype was determined by performing allele-specific droplet digital polymerase chain reaction (ddPCR) using the TaqMan array for CD16 (rs396991; Life Technologies, Carlsbad, CA) [18]. A master reaction mix was prepared, and 1 µL of DNA was added. The PCR reaction was performed as previously described [3].

Statistical analyses

Statistical analyses were performed using GraphPad Prism 6 (GraphPad Software, La Jolla, CA), and p -values were calculated using the Wilcoxon matched-pairs signed rank test. For the flow cytometry analysis, due to the large number of tests performed, p -values were adjusted using Holm's method (step-down Bonferroni), as previously described [15, 19]. The adjustment was made for the number of subsets with a frequency above 0.01% of PBMC ($n = 9$ for classic subsets, $n = 29$ for subsets in CD4⁺ T cells, $n = 25$ for CD8⁺ T cells, $n = 5$ for Tregs, $n = 14$ for NK cells, $n = 3$ for NK-T cells, $n = 4$ for B cells, $n = 2$ for cDCs, $n = 3$ for pDCs, $n = 15$ for MDSC). Subsets with a potentially biologically relevant change were defined as subsets with a Holm adjusted $p < 0.05$,



majority of patients >25% change, difference in medians of pre- vs. post-therapy >0.01% of PBMC, and a frequency >0.01% of PBMC. Trends were defined as subsets with an unadjusted $p < 0.05$, along with the additional criteria used to define changes.

Results

To interrogate any potential effects of the anti-PD-L1 monoclonal (avelumab) on immune cells in cancer patients, we employed five panels of antibodies in flow cytometry analyses to define 123 different immune cell subsets. The antibody panels used are shown in Additional file 1: Table S1. The complete list of subsets analyzed is shown in Table 1. Additional file 1: Table S2 shows the “classic” immune cell types (CD4⁺ and CD8⁺ T cells, T regulatory cells (Tregs), B cells, NK cells, NK-T cells, cDC, pDC, MDSC) and the various markers used to identify the “refined” subsets within each classic cell type, along with a brief description of what is generally known about each subset. Figure 1 shows an example of the flow cytometry gating strategy employed in these studies using PBMC from a cancer patient following nine cycles of avelumab to identify the 123 immune cell subsets.

As the ability to correctly detect and enumerate PD-L1 positive immune cells is fundamental for this study, experiments were performed to ensure that PD-L1 positive cells could be correctly identified in the staining and gating schema. PBMC from a healthy donor were stained with PD-L1 alone, as well as with multiparametric stains of PD-L1 in each of the five staining panels, and assessed for PD-L1 surface expression, with fluorescence minus one (FMO) controls used for gating. Total PBMC, as well as those in the lymphocyte-monocyte region and non-lymphocyte-monocyte region, expressed a similar frequency of PD-L1 when cells were stained with PD-L1 alone, or PD-L1 in the multiparametric stains, demonstrating that this antibody is compatible in combination with the other antibodies that are needed to identify the various immune cell subsets (Additional file 2: Figure S2). In addition, experiments were undertaken to ensure that the PD-L1 clone used to detect surface PD-L1 in the various immune cell subsets was not blocked by the potential binding of avelumab to the immune cells. PBMC were pre-incubated for 30 min with avelumab or an IgG1 control (0.2, 2, and 20 $\mu\text{g}/\text{mL}$), and then stained with the antibody panels to detect PD-L1 expression in the various immune cell subsets. As seen in Additional file 2: Table S3, PD-L1 was detectable, and measured at a very similar frequency within immune cell subsets (data shown of CD4, CD8, cDC and B cells, both as a percentage of parent and percentage of total PBMC), regardless of whether the PBMC were pre-incubated with the IgG1 isotype control or avelumab. These results demonstrate that the PD-L1 clone (MIH-1) used in the present study to assess surface

expression of PD-L1 does not compete for binding with avelumab in PBMC, and can thus be used to measure PD-L1 expression in patients treated with avelumab.

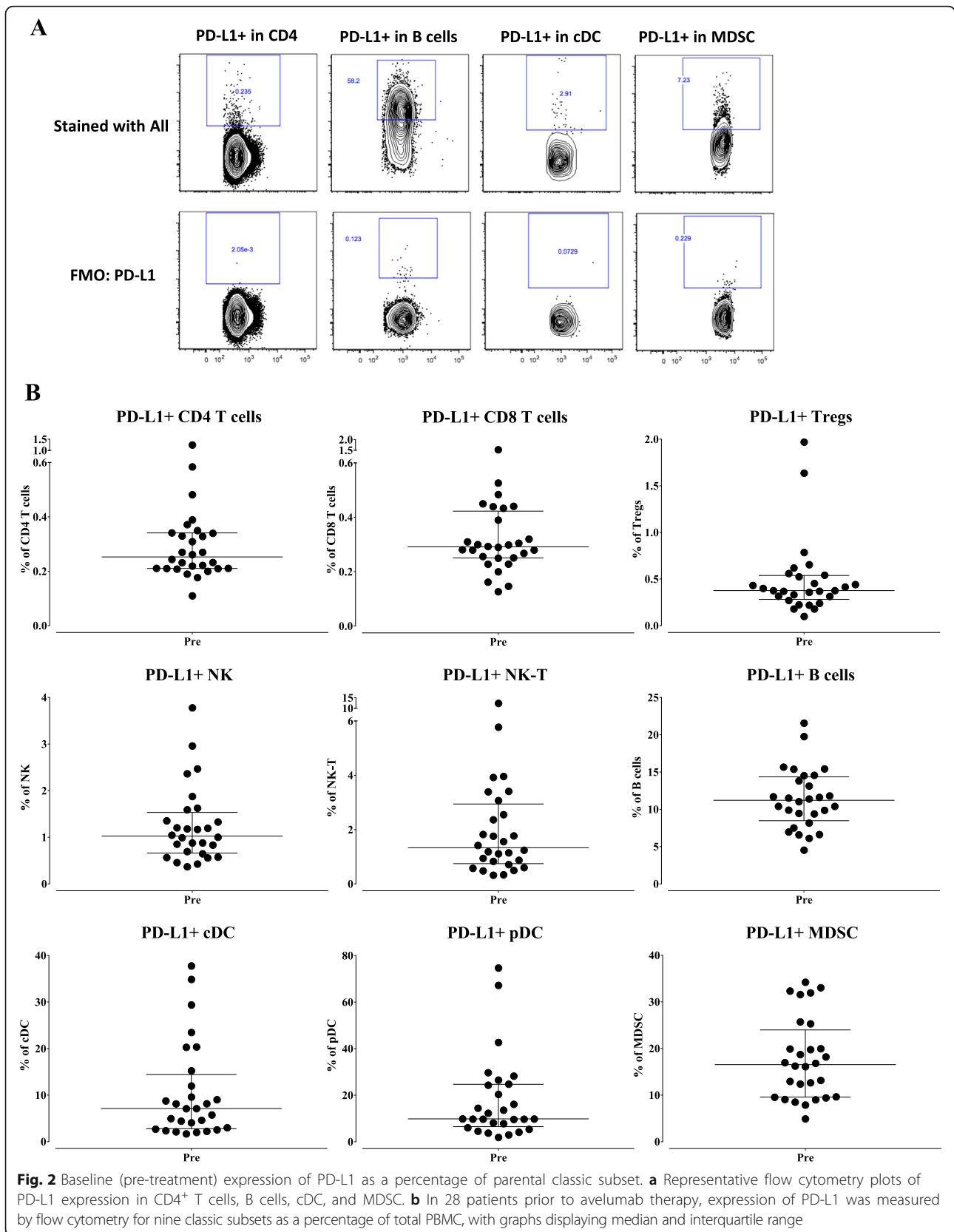
PBMC from 28 patients in the Phase I trial were first analyzed at baseline (prior to receiving avelumab) for the surface expression of PD-L1 on each of the nine classic cell types and 16 refined subsets. Table 2 shows the median percentage of each cell type expressing PD-L1, both as a percentage of total PBMC as well as a percentage of the parental cell type. Representative flow cytometry plots of PD-L1 within CD4⁺ T cells, B cells, cDC and MDSC, as well as FMO control used for gating, are shown in Fig. 2a. Figure 2b shows the range at baseline of expression of PD-L1 on the nine classic cell types as a

Table 2 Baseline expression of PD-L1

Classic subsets	Refined subsets	Median % PBMC	Median % parent
PD-L1 ⁺ CD4		0.08	0.25
	PD-L1 ⁺ ICOS ⁺ CD4	0.05	0.81
	PD-L1 ⁺ naïve CD4	0.01	0.26
	PD-L1 ⁺ CM CD4	0.02	0.28
	PD-L1 ⁺ EM CD4	0.06	0.31
PD-L1 ⁺ EMRA CD4		0.01	0.35
		0.04	0.29
	PD-L1 ⁺ naïve CD8	<0.01	0.40
	PD-L1 ⁺ CM CD8	<0.01	0.41
PD-L1 ⁺ EM CD8		0.02	0.26
	PD-L1 ⁺ EMRA CD8	0.01	0.30
	PD-L1 ⁺ Tregs	<0.01	0.38
PD-L1 ⁺ NK		0.06	1.03
	PD-L1 ⁺ mature NK	0.04	0.97
	PD-L1 ⁺ functional intermediate NK	<0.01	0.31
	PD-L1 ⁺ immature NK	<0.01	0.66
PD-L1 ⁺ unconventional NK		0.02	5.58
		0.03	1.34
PD-L1 ⁺ NK-T		0.88	11.22
PD-L1 ⁺ B cells		0.02	7.12
PD-L1 ⁺ cDC		0.02	9.85
PD-L1 ⁺ pDC		0.71	16.54
PD-L1 ⁺ MDSC		0.10	4.81
	PD-L1 ⁺ mMDSC	0.26	35.77
	PD-L1 ⁺ gMDSC	0.17	18.75

In 28 patients prior to avelumab therapy, expression of PD-L1 was measured by flow cytometry in 9 classic subsets and 16 refined subsets as both percentage of total PBMC and of parental cell type

cDC conventional dendritic cells, CM central memory, EM effector memory, EMRA terminally differentiated effector memory, gMDSC granulocytic MDSC, ICOS inducible T cell co-stimulator, *lin neg MDSCs* lineage negative MDSCs, MDSC myeloid derived suppressor cell, mMDSC monocytic MDSC, NK natural killer, pDC plasmacytoid DC, PD-L1 programmed cell death ligand-1, Tregs regulatory T cells



percentage of each classic parental subset, and Fig. 3 shows the range of expression at baseline of PD-L1 of a given cell type as a percentage of total PBMC. For example, while only 0.1 to 3% of PBMC are PD-L1⁺ MDSC (Fig. 3, lower right panel), 5 to 35% of MDSC express PD-L1 (Fig. 2b, lower right panel). Also shown is the variation in PD-L1 expression amongst the parental immune cell types with the highest level of expression of PD-L1 seen on B cells and MDSC (Fig. 3).

Changes in the levels of PD-L1 expressing cells in PBMC were then evaluated after patients received one, three and nine cycles of avelumab every 2 weeks. Using the criteria of a Holm adjusted *p*-value as detailed in the Methods section, there were no significant changes in any of the nine classic immune cell types, or in the PD-L1 expressing classic cell subsets following one, three or nine cycles of avelumab. No differences were seen in results after one or three cycles of avelumab; thus only

the results after one cycle and nine cycles are shown; data following three cycles of avelumab is available in Additional file 1: Table S4. Table 3A shows the percentage of patients who had an increase of more than 25%, a minimal change (change less than the 25% cutoff), or a decrease of more than 25% in the nine classic cell types after one or nine cycles of avelumab. There were some trends in classic cell types expressing PD-L1 after nine bi-weekly cycles of avelumab (Table 3B); there was an increase in some patients of PD-L1⁺ pDC and PD-L1⁺ MDSC. None of these trends, however, met statistical significance using the Holm adjusted criteria. We also evaluated additional refined subsets expressing PD-L1 for changes after one, three and nine cycles of avelumab. Only one PD-L1⁺ refined subset met statistical significance using the Holm adjusted criteria, and this change (an increase) only occurred following nine cycles of avelumab (PD-L1⁺ lineage negative MDSC, Holm adjusted

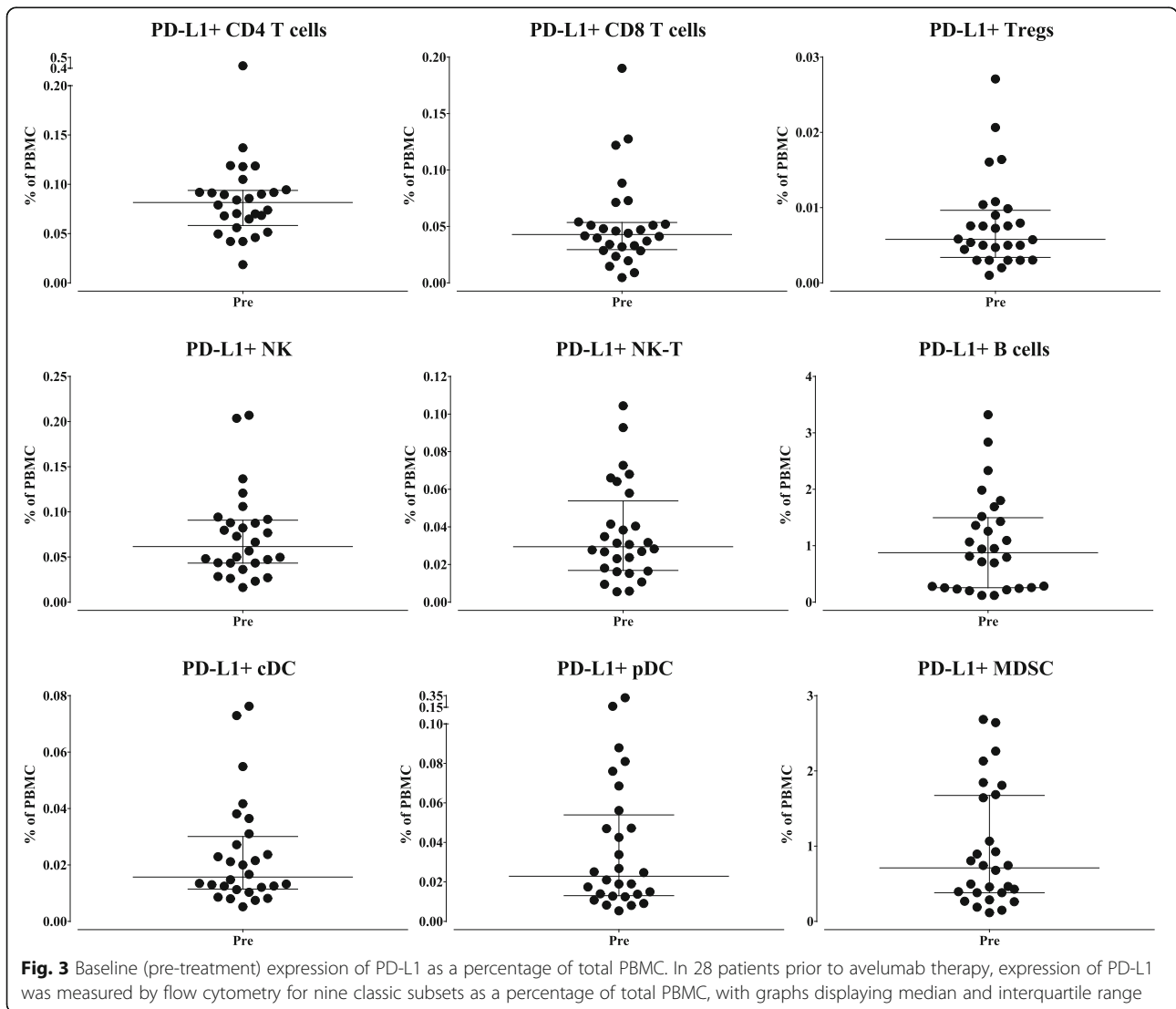


Table 3 Effect of avelumab on classic and PD-L1⁺ classic immune cell subsets

Subset	Pre vs 1 cycle				Pre vs 9 cycles			
	Increase	Minimal change	Decrease	<i>P</i> -value	Increase	Minimal change	Decrease	<i>P</i> -value
A. Classic subsets								
CD4	0 (0%)	18 (95%)	1 (5%)	0.0230 (↑ [^] , 0.2070)	0 (0%)	12 (75%)	4 (25%)	0.0063 (↓ [^] , 0.0567)
CD8	1 (5%)	16 (84%)	2 (11%)	0.1447 (=)	3 (19%)	11 (68%)	2 (13%)	0.9799 (=)
Tregs	7 (37%)	10 (53%)	2 (10%)	0.2253 (=)	2 (12%)	7 (44%)	7 (44%)	0.0934 (=)
NK	5 (26%)	10 (53%)	4 (21%)	0.8288 (=)	0 (0%)	9 (56%)	7 (44%)	0.0182 (↓ [^] , 0.1456)
NK-T	2 (11%)	15 (78%)	2 (11%)	0.2413 (=)	1 (6%)	12 (75%)	3 (19%)	0.1046 (=)
B cells	5 (26%)	12 (63%)	2 (11%)	0.7381 (=)	6 (38%)	5 (31%)	5 (31%)	0.8209 (=)
cDC	3 (16%)	15 (79%)	1 (5%)	0.3955 (=)	6 (37%)	7 (44%)	3 (19%)	0.7436 (=)
pDC	6 (32%)	8 (42%)	5 (26%)	0.4900 (=)	6 (38%)	9 (56%)	1 (6%)	0.0833 (=)
MDSC	8 (42%)	8 (42%)	3 (16%)	0.1232 (=)	8 (50%)	7 (44%)	1 (6%)	0.0833 (=)
B. PD-L1 ⁺ classic subsets								
PD-L1 ⁺ CD4	5 (26%)	9 (48%)	5 (26%)	0.9843 (=)	3 (19%)	9 (56%)	4 (25%)	0.9999 (=)
PD-L1 ⁺ CD8	4 (21%)	9 (47%)	6 (32%)	0.1688 (=)	4 (25%)	9 (56%)	3 (19%)	0.9999 (=)
PD-L1 ⁺ Treg	n/a	n/a	n/a	n/a	n/a	n/a	n/a	n/a
PD-L1 ⁺ NK	5 (26%)	6 (32%)	8 (42%)	0.4180 (=)	7 (44%)	7 (44%)	2 (12%)	0.1046 (=)
PD-L1 ⁺ NK-T	5 (26%)	8 (42%)	6 (32%)	0.4900 (=)	6 (38%)	6 (38%)	4 (24%)	0.1439 (=)
PD-L1 ⁺ B cells	9 (47%)	6 (32%)	4 (21%)	0.6507 (=)	6 (37%)	7 (44%)	3 (19%)	0.5282 (=)
PD-L1 ⁺ cDC	5 (26%)	8 (42%)	6 (32%)	0.3736 (=)	2 (13%)	4 (25%)	10 (62%)	0.0386 (↓ [*] , 0.0772)
PD-L1 ⁺ pDC	3 (16%)	2 (10%)	14 (74%)	0.0258 (↓ [*] , 0.0774)	10 (63%)	1 (6%)	5 (31%)	0.0443 (↑, 0.1005)
PD-L1 ⁺ MDSC	8 (42%)	6 (32%)	5 (26%)	0.6507 (=)	10 (63%)	4 (25%)	2 (12%)	0.0131 (↑, 0.1703)

Classic subsets (A) and PD-L1⁺ classic subsets (B) were examined pre-therapy and post-1 cycle ($n = 19$) and 9 cycles ($n = 16$) of avelumab. Results are displayed as the number of patients (percentage of total patients) with an increase of more than 25%, minimal change of less than 25%, and a decrease of more than 25% compared to pre-therapy. Unadjusted p -values (= indicates no change; arrows indicate direction of change compared to pre-therapy; and Holm adjusted p -value is listed for subsets with significant unadjusted p -value) were calculated using the Wilcoxon matched-pairs signed rank test. n/a = not applicable as frequency of subset <0.01% PBMC; [^] = majority of patients with minimal change; * = difference in medians pre- vs post-therapy < 0.01

cDC conventional dendritic cells, MDSC myeloid derived suppressor cell, NK natural killer, pDC plasmacytoid DC, PBMC peripheral blood mononuclear cell, Tregs regulatory T cells

$p = 0.0015$) (Additional file 1: Table S5). We also evaluated an additional 89 refined immune cell subsets relating to maturation and function. Table 4 shows the subsets that met the criteria for a trend (unadjusted p -value) at any dose; however, none met statistical significance for a change (Holm adjusted p -value). Representative graphs show degree of change in subsets meeting the trend criteria in patients receiving one cycle of 1, 3, 10, or 20 mg/kg of avelumab (Fig. 4). Trends in change from baseline were seen in more cell types after nine cycles of avelumab vs. one or three cycles (Table 4). Since these were patients with metastatic disease, these changes could be due to disease progression; however, none were statistically significant using the Holm adjusted p -value (Table 4).

We also conducted additional studies using autologous PBMC from healthy donors as targets to determine if avelumab would mediate ADCC of PBMC using NK cells as effectors. We have previously shown [3] that avelumab can mediate ADCC against the human lung cancer line H441; thus it was used as a positive control. As seen in Fig. 5a, 100% of H441 tumor cells express PD-

L1, the target of avelumab. Using NK cells isolated from five healthy donors as effector cells, avelumab mediated appreciable ADCC of H441 target cells at multiple effector to target ratios compared to the isotype control MAb (which denotes endogenous NK lysis) (Fig. 5b). Using the same healthy donor NK cells with avelumab, no lysis of autologous PBMC was seen; however, due to the sensitivity of the assay, one cannot rule out the lysis of a minor subpopulation of cells that express PD-L1.

Studies were performed to address the concern of the ADCC assay sensitivity, as well as to investigate the ability of cancer patient NK cells to mediate ADCC of PD-L1 expressing targets. NK cells were isolated from a metastatic cancer patient with NSCLC, and tested for their ability to induce avelumab mediated ADCC against autologous PBMC that were sorted to enrich for PD-L1 positive and negative subsets. As seen in Fig. 6a, compared to total PBMC, in which 17% of cells were positive for PD-L1, expression of PD-L1 was negligible (<1% positive) in the PD-L1 negative sorted fraction and markedly enriched in the PD-L1 positive sorted fraction

Table 4 Effect of avelumab on 89 refined immune cell subsets

Post	Subset	Increase	Minimal change	Decrease	Unadjusted <i>P</i> -value	Direction	Holm adjusted <i>P</i> -value
1 cycle	PD-1 ⁺ ICOS ⁺ CD4	12 (63%)	5 (26%)	2 (11%)	0.0181	↑	0.5611
	PD-1 ⁺ Tregs	12 (63%)	5 (26%)	2 (11%)	0.0141	↑	0.0705
	Functional intermediate NK	10 (53%)	6 (31%)	3 (16%)	0.0401	↑	0.5213
3 cycles	Functional intermediate NK	1 (7%)	4 (29%)	9 (64%)	0.0295	↓	0.4130
9 cycles	CTLA-4 ⁺ EM CD8	9 (56%)	6 (38%)	1 (6%)	0.0250	↑	0.6250
	Functional intermediate NK	2 (12%)	4 (25%)	10 (63%)	0.0386	↓	0.5018
	PD-1 ⁺ pDC	10 (63%)	2 (12%)	4 (25%)	0.0335	↑	0.1005
	CD16 ⁺ MDSC	9 (56%)	5 (31%)	2 (13%)	0.0092	↑	0.1288
	gMDSC	11 (69%)	2 (12%)	3 (19%)	0.0131	↑	0.1703
	CD16 ⁺ gMDSC	10 (62%)	3 (19%)	3 (19%)	0.0155	↑	0.1705
	PD-1 ⁺ lin neg MDSC	10 (62%)	4 (25%)	2 (13%)	0.0182	↑	0.1820

The frequency of 89 refined immune cell subsets was examined pre-therapy and post-1 cycle (*n*=19), 3 cycles (*n*=14), and 9 cycles (*n*=16) of avelumab. Table displays subsets that met criteria as a potentially biologically relevant trend. Results are displayed as the number of patients (percentage of total patients) with an increase of more than 25%, minimal change of less than 25%, and a decrease of more than 25% compared to pre-therapy. Unadjusted *p*-values (direction of change compared to pre-therapy) were calculated using the Wilcoxon matched-pairs signed rank test, and Holm adjustment was made for the number of subsets within the classic subsets with a frequency above 0.01% of PBMC
EM effector memory, *gMDSC* granulocytic MDSC, *ICOS* inducible T cell co-stimulator, *lin neg MDSC* lineage negative MDSC, *MDSC* myeloid derived suppressor cell, *NK* natural killer, *pDC* plasmacytoid DC, *PD-1* programmed cell death protein 1, *Tregs* regulatory T cells

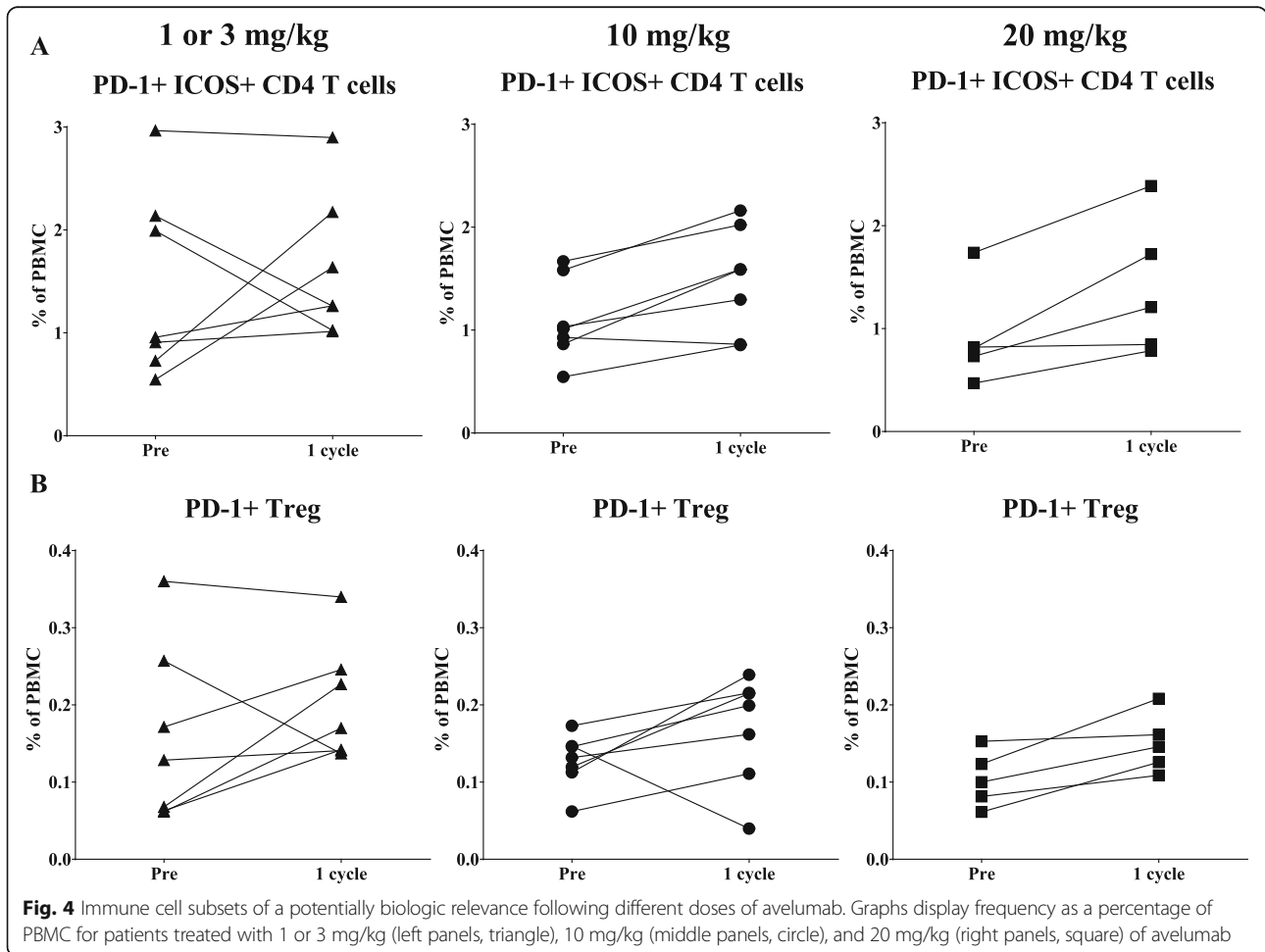
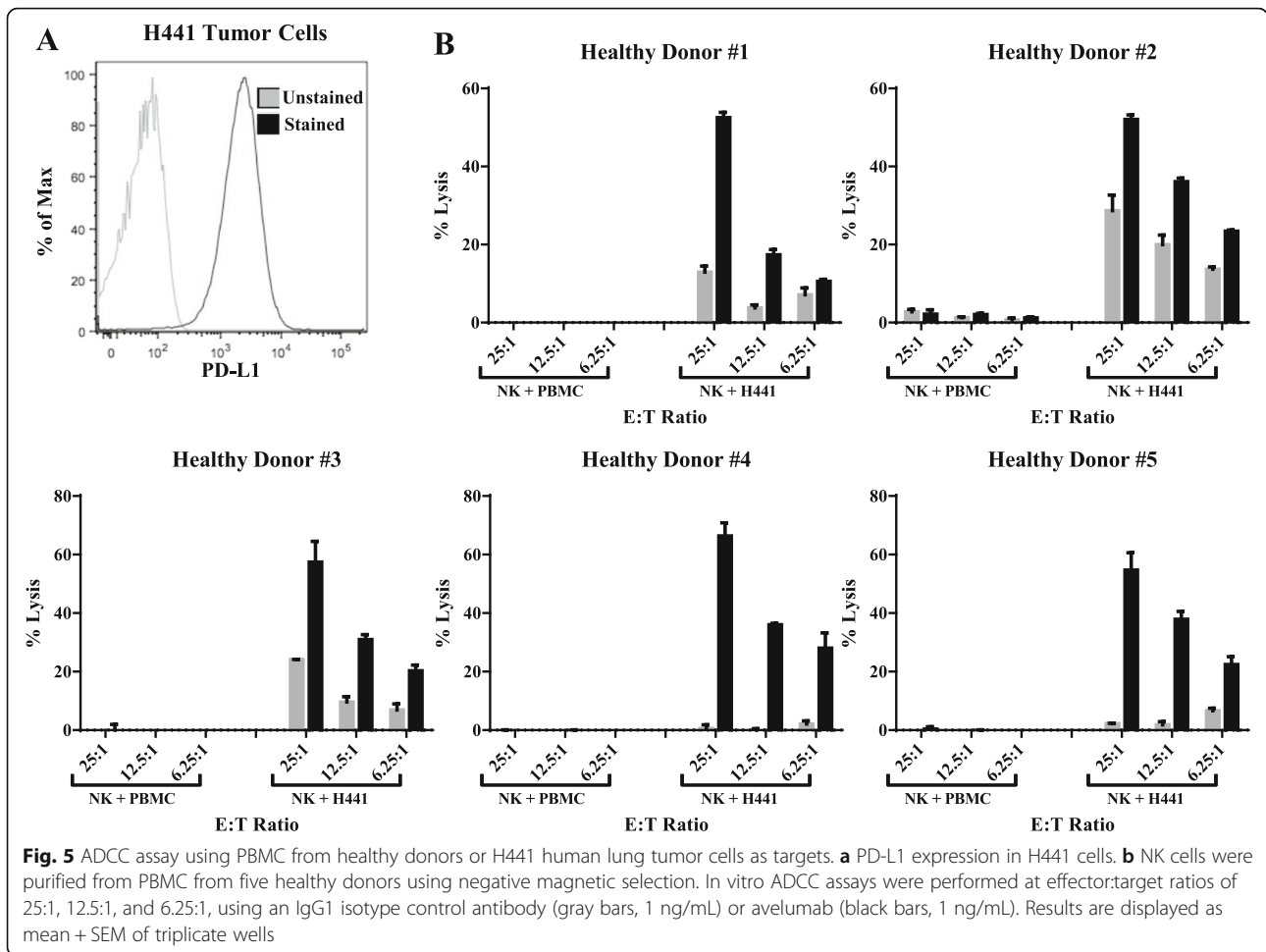


Fig. 4 Immune cell subsets of a potentially biologic relevance following different doses of avelumab. Graphs display frequency as a percentage of PBMC for patients treated with 1 or 3 mg/kg (left panels, triangle), 10 mg/kg (middle panels, circle), and 20 mg/kg (right panels, square) of avelumab



(74% positive). Human lung cancer lines in which 76% of cells expressed PD-L1 (H460) and 100% of cells expressed PD-L1 (H441) were used as positive controls (Fig. 6b). Here, using NK cells from a cancer patient as effector cells, avelumab mediated appreciable ADCC of both H460 and H441 target cells at an effector:target ratio of 25:1 compared to the isotype control MAb; however, using the same patient's NK cells with avelumab, no lysis of either total, PD-L1 negative, or PD-L1 positive enriched PBMC was detected (Fig. 6c). Similar results were observed with NK cells from two additional cancer patients (data not shown). Notably, the expression of PD-L1 in the positively sorted fraction of cancer patient PBMC (both % and MFI) was similar to that of the H460 cells, but less than that seen in the H441 cells (Fig. 6d).

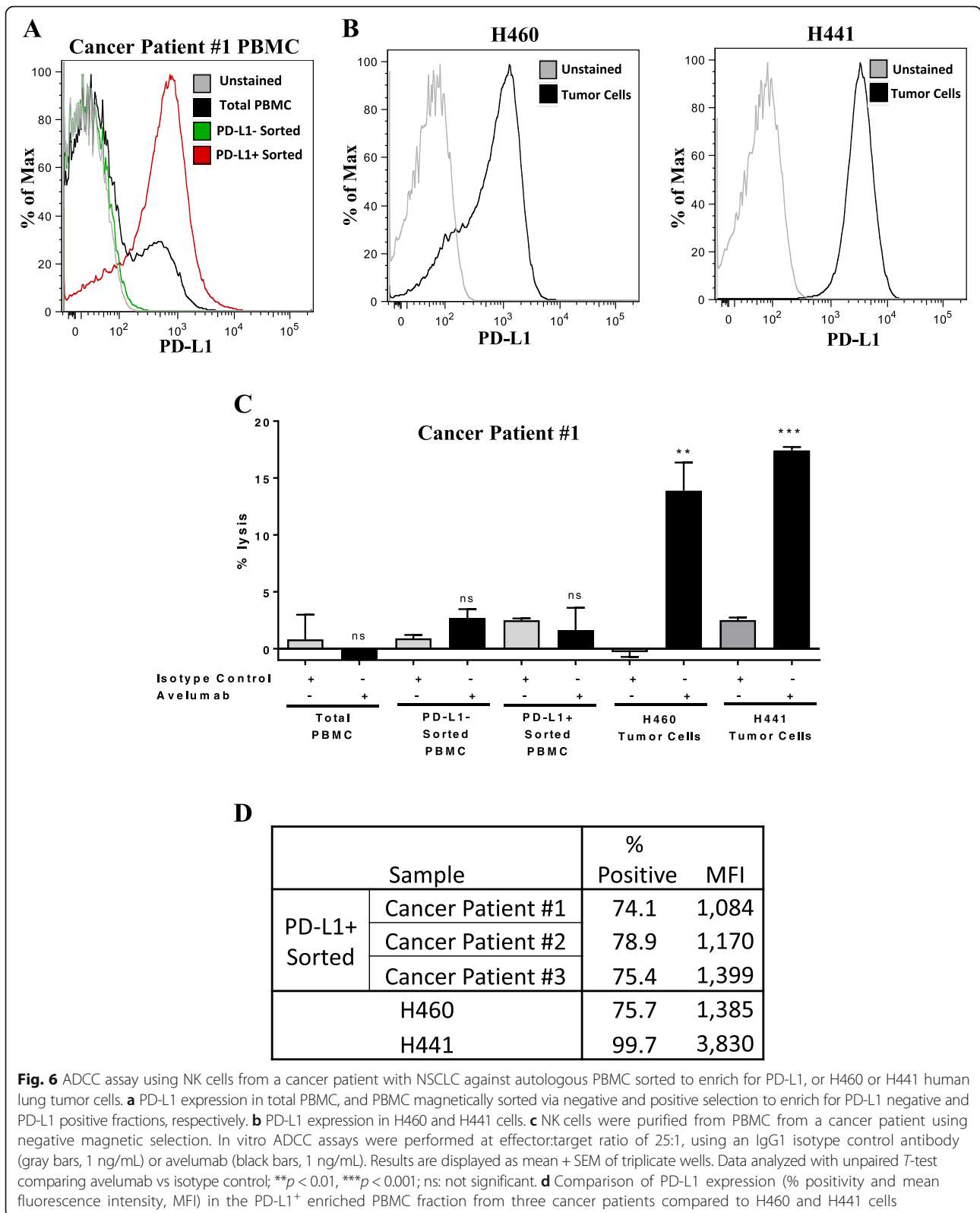
As NK CD16 polymorphism has been shown [20] to contribute to the variability of the level of ADCC mediated by NK cells, the genotype of the NK CD16 used as effectors was examined for the healthy donors in these experiments. Four of the five healthy donors used in the in vitro ADCC assay had the V/F genotype, while one had the F/F genotype; the genotype of the cancer

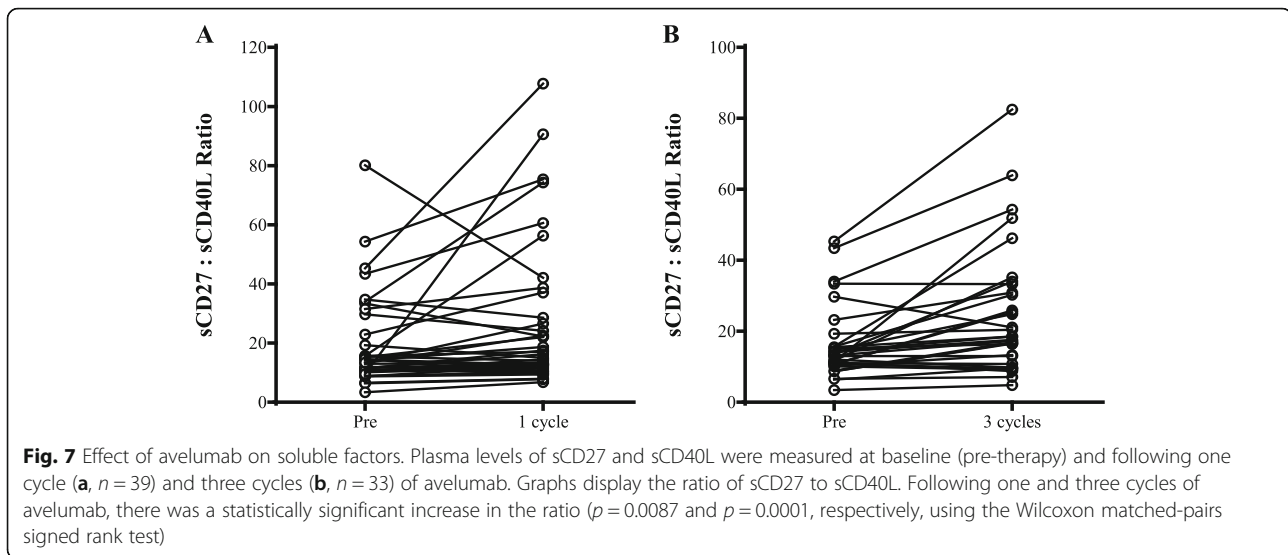
patients used in vitro ADCC assays is unknown. The genotypes of 25 of the 28 patients treated with avelumab that were assessed by flow cytometry were determined; 12 patients had the F/F genotype, 11 had the V/F genotype, and 2 had the V/V genotype.

We have previously shown [21, 22] that sCD27 in serum is a marker of T-cell activation and sCD40L in serum is an indicator of immune suppression. Preliminary data has also suggested that increases in the ratio of sCD27:sCD40L correlate with improved patient outcome in some immunotherapy trials. As seen in Fig. 7, there were statistical increases in the sCD27:sCD40L ratio after one administration and three administrations of avelumab ($p = 0.0087$ and $p = 0.0001$, respectively).

Discussion

The limited toxicity observed in the dose escalation Phase I trial and Phase II trials, and the results described here on the minimal effect of avelumab on 123 immune cell subsets of patients receiving avelumab should help reduce concern about the use of a fully human IgG1 directed against PD-L1. It should be noted that several





widely used and effective anti-cancer MABs, including trastuzumab (Herceptin), cetuximab (Erbix), and rituximab (Rituxan), are all of the same human IgG1 isotype. While the targets for each of these MABs are also expressed on some normal tissues, their clinical effectiveness has been shown to outweigh toxicities. The actual mode of action of trastuzumab, cetuximab, and rituximab is generally accepted to be due to the reactivity of each MAB to its respective receptor on tumor cells; evidence also exists, however, that some anti-tumor activity of each of these three antibodies may be due to ADCC. It is known that human NK cells possessing the high affinity V/V CD16 allele generally have more potent ADCC activity than NK cells possessing the lower affinity F/F or V/F CD16 alleles. It has been shown in some prior clinical studies that patients expressing the V/V CD16 allele have greater clinical benefit, when receiving trastuzumab, cetuximab or rituximab, than those patients with the V/F or F/F allele [20, 23]. The genotype of the CD16 allele was assessed in patients of the current Phase I dose escalation trial of avelumab, and the V/V genotype was rarely identified (2/25 patients). In future randomized trials of avelumab, studies will be carried out to determine if clinical benefit of avelumab correlates with the V/V CD16 allele on NK cells.

An anti-PD-L1 MAB of the IgG1 isotype also enables the potential for enhanced ADCC activity by employing agents such as IL-15 and IL-12 immunocytokines. Recent preclinical and clinical studies with recombinant IL-15 [24, 25] and an IL-15/Ra/Fc immunocytokine [26, 27] have shown that these agents greatly enhance the level of NK cells as well as the lytic activity of NK cells on a per cell basis. In vitro studies have shown that IL-12 also enhances NK-mediated ADCC employing avelumab [3]. A tumor targeting IL-12 immunocytokine,

designated NHS-IL-12, is currently in clinical studies and may be of use toward this goal. The use in adoptive transfer of allogeneic NK cells (NK-92) has previously been shown to be safe with evidence of clinical activity; a variant of NK-92 genetically engineered to express both IL-2 (and consequent high levels of granzyme) and the high affinity CD16 V/V allele has now been shown to greatly enhance the ADCC activity of avelumab [manuscript submitted for publication]. Since only approximately 10% of humans endogenously express the V/V allele [28], the adoptive transfer of these CD16 high affinity NK (haNK) cells in combination with avelumab merits further investigation.

Analyses of the 123 immune subsets in the periphery also have other potential applications. It has recently been shown [29] that analyses of refined peripheral immune cell subsets in patients from two randomized trials, prior to the initiation of immunotherapy, were able to predict, with statistical significance, those patients more likely to benefit clinically. This was not the case when classic immune cell subsets were analyzed in an identical manner. Results from these two randomized trials showed that the analyses of refined cell subsets did not predict patient benefit in the arms of the trials in which patients received chemotherapy alone or radionuclide alone, but only predicted benefit in the arms of the trials in which patients received vaccine plus chemotherapy or vaccine plus radionuclide. The analyses of immune cell subsets in the periphery, prior to the initiation of immunotherapy, have also been reported by several groups to be a potential indicator of those patients most likely to achieve clinical benefit [30, 31]. While it is clear that analysis of biopsies for the presence of immune infiltrate has been shown in some cases to be an important predictor of clinical benefit, especially in the

analyses of biopsies of primary lesions of colorectal cancer patients [32], the metastatic lesions of many cancer types are not always amenable to biopsy. Moreover, it is known that there is often an interplay between different immune cell types. The analyses of the 123 immune cell subsets in the periphery could add potentially valuable information to that obtained in analyses of available biopsy specimens; thus the dual analyses of specific immune subsets in tumor and in the periphery may be of optimal benefit in helping to define patient outcome. Assessment of soluble factors in sera or plasma that can easily be tracked in patients over time can also provide an overall indication of the immune environment induced following a given therapy. In the present study, exposure to avelumab significantly increased the ratio of sCD27/sCD40L. Previous studies [21, 22] have found that sCD27 is a marker of T-cell activation, while sCD40L is a measure of immune suppression, and that increases and decreases, respectively in these measures in patient serum/plasma, correlate with improved outcome in some immunotherapy trials. Future studies of avelumab in expansion cohorts will assess if there is any link between clinical efficacy and the trends of changes in soluble factors (increase in the ratio of sCD27/sCD40L) and specific peripheral immune cell subsets.

It is understood that there are a number of limitations in the current study. PD-L1, for example, is expressed at a low level in many immune cell types in the periphery; however, as seen in Fig. 2b, there are some subsets such as dendritic cells, B cells, and MDSCs that were identified as expressing higher levels of this marker. In addition, it has been reported that cryopreservation may impact PD-L1 expression, reducing expression on monocytes and CD8⁺ T cells, but not on CD4⁺ T cells [33]. However, because of the need to analyze clinical trial samples in batches (pre- and all post-treatment samples from the same patient assayed at the same time) to reduce other experimental variables, the present study assessed cryopreserved material. Importantly, PBMC samples pre- and post-treatment were isolated and cryopreserved in the same manner following stringent protocols, and a live/dead discriminator was used to exclude dead cells that bind non-specifically to antibody. It is also recognized that PD-L1 expression can be temporally influenced by therapies that induce immune activation, and that expression of immune cells in the periphery may likely differ from what is seen within the tumor. Despite all of these limitations, we show that there is no marked loss of PD-L1 expressing immune cells in the peripheral blood of patients treated with avelumab. Studies are planned to examine the immune effects of avelumab within the tumor microenvironment in future expansion cohorts of avelumab in patients with tumors that can be biopsied, where PD-L1 may be more broadly

expressed and upregulated on immune cells by the immune potentiating properties of avelumab.

NK cells are known to express numerous Ig-like receptors and C-type lectin receptors that deliver a finely tuned balance of activating and inhibitory signals that can influence their ability to discriminate between self/healthy cells from transformed/pathogen infected cells [34]. We demonstrate in the present study that NK cells isolated from metastatic NSCLC patients induce avelumab mediated ADCC of human lung tumor cell lines but not of autologous PBMC, including those that have been sorted to enrich for expression of PD-L1, the target of avelumab. This is in concordance with the finding of Voskens et al. [35], that ex vivo expanded human NK cells expressing high levels of activating receptors can mediate cytotoxicity of cancer cell lines by direct recognition and ADCC, but do not lyse autologous PBMC. In that study it was postulated that the inhibitory ligands expressed on normal PBMC may predominate over activating signals, in order to be able to control the NK-mediated cytolytic activity against non-malignant cells.

Conclusions

In conclusion, our data show a lack of any significant effect on 123 peripheral immune cell subsets, including those that express PD-L1, following treatment of cancer patients with multiple cycles of avelumab. We also demonstrate in controlled in vitro experiments that avelumab can mediate ADCC of PD-L1 expressing tumor cells, but not against PD-L1 expressing immune cells. These findings complement the limited toxicity observed in the dose escalation Phase I and Phase II trials of avelumab, and should help to reduce concern about the use of a fully human IgG1 MAb directed against PD-L1. This study also supports the rationale to further exploit the potential ADCC mechanism of action of avelumab against tumor cells to potentially enhance clinical activity.

Additional files

Additional file 1: Table S1. Antibodies used for 5 panel stain to identify 123 peripheral immune cell subsets. Panel 1: PD-1 signaling; Panel 2: CD4⁺ T cells, CD8⁺ T cells, B cells; Panel 3: Tregs; Panel 4: NK, NK-T, cDC, pDC; Panel 5: MDSC. **Table S2.** Peripheral immune cell subsets analyzed by flow cytometry. Analysis of 123 subsets using 30 unique markers. **Table S3.** PD-L1 clone MIH-1 used to detect surface expression of PD-L1 in immune cell subsets does not compete for binding with avelumab. **Table S4.** Effect of three cycles of avelumab on classic and PD-L1⁺ classic immune cell subsets. Classic and PD-L1⁺ classic subsets were examined pre-therapy and post-three cycles ($n = 14$) of avelumab. **Table S5.** Effect of avelumab on PD-L1⁺ refined immune cell subsets. PD-L1⁺ refined subsets were examined pre-therapy and post-one cycle ($n = 19$), three cycles ($n = 14$), and nine cycles ($n = 16$) of avelumab. (PDF 464 kb)

Additional file 2: Figure S1. Configuration of LSR II to allow for the detection of up to 11 markers per staining panel. **Figure S2.** PD-L1 expression in PBMC from a healthy donor stained with single and multiparametric stains of PD-L1. (PDF 520 kb)

Abbreviations

ADCC: Antibody-dependent cell-mediated cytotoxicity; cDC: Conventional dendritic cells; ddPCR: Droplet digital polymerase chain reaction; DLT: Dose-limiting toxicities; F: Phenylalanine; FMO: Fluorescence minus one; MAb: Monoclonal antibody; mCRPC: Metastatic castration resistant prostate cancer; MDSC: Myeloid derived suppressor cells; MFI: Mean fluorescence intensity; NK: Natural killer; NSCLC: Non-small cell lung cancer; PBMC: Peripheral blood mononuclear cells; PD-1: Programmed cell death protein 1; pDC: Plasmacytoid dendritic cells; PD-L1: Programmed cell death protein-1 ligand; sCD27: Soluble CD27; sCD40L: Soluble CD40 ligand; Tregs: Regulatory T cells; V: Valine

Acknowledgments

The authors thank Debra Weingarten for her editorial assistance in the preparation of this manuscript.

Funding

This research was supported by the Intramural Research Program of the Center for Cancer Research, National Cancer Institute (NCI), National Institutes of Health, and via a Cooperative Research and Development Agreement (CRADA) between EMD Serono and the NCI.

Availability of data and materials

N/A.

Authors' contributions

Conception and design: RND, JLG, JS. Acquisition of data: RND, LML, IG, CJ, MF, CRH, JLG, JS. Analysis and interpretation of data: RND, LML, IG, CJ, MF, JS. Manuscript preparation and writing: LML, RND, JS. Manuscript review: RND, LML, IG, CJ, MF, RAM, CRH, JLG, JS. All authors read and approved the final manuscript and agreed to be accountable for the work.

Competing interests

The authors declare that they have no competing interests.

Consent for publication

N/A.

Ethics approval and consent to participate

The National Cancer Institute Institutional Review Board approved the trial procedures and informed consent was obtained in accordance with the Declaration of Helsinki.

Author details

¹Laboratory of Tumor Immunology and Biology, Center for Cancer Research, National Cancer Institute, National Institutes of Health, 10 Center Drive, Room 8B09, Bethesda, MD, USA. ²Genitourinary Malignancies Branch, Center for Cancer Research, National Cancer Institute, National Institutes of Health, Bethesda, MD, USA.

Received: 7 November 2016 Accepted: 1 February 2017

Published online: 21 February 2017

References

- Callahan MK, et al. Targeting T cell co-receptors for cancer therapy. *Immunity*. 2016;44:1069–78.
- Hoos A. Development of immuno-oncology drugs - from CTLA4 to PD1 to the next generations. *Nat Rev Drug Discov*. 2016;15:235–47.
- Boyerinas B, et al. Antibody-dependent cellular cytotoxicity activity of a novel anti-PD-L1 antibody avelumab (MSB0010718C) on human tumor cells. *Cancer Immunol Res*. 2015;3:1148–57.
- Fujii R, et al. Enhanced killing of chordoma cells by antibody-dependent cell-mediated cytotoxicity employing the novel anti-PD-L1 antibody avelumab. *Oncotarget*. 2016;7:33498–511.
- Khanna S, et al. Malignant mesothelioma effusions are infiltrated by CD3+ T cells highly expressing PD-L1 and the PD-L1+ tumor cells within these effusions are susceptible to ADCC by the anti-PD-L1 antibody avelumab. *J Thorac Oncol*. 2016;11:1993–200.
- Vanderveer AJ, et al. Systemic immunotherapy of non-muscle invasive mouse bladder cancer with avelumab, an anti-PD-L1 immune checkpoint inhibitor. *Cancer Immunol Res*. 2016;4:452–62.
- Grenga I, et al. A fully human IgG1 anti-PD-L1 MAb in an in vitro assay enhances antigen-specific T-cell responses. *Clin Transl Immunol*. 2016;5:e83.
- Cheol Chung H, et al. Avelumab (MSB0010718C; anti-PD-L1) in patients with advanced gastric or gastroesophageal junction cancer from the JAVELIN solid tumor phase Ib trial: Analysis of safety and clinical activity. American Society of Clinical Oncology 2016 Annual Meeting. *J Clin Oncol*. 2016;34 (suppl; abstr 4009).
- Disis ML, et al. Avelumab (MSB0010718C; anti-PD-L1) in patients with recurrent/refractory ovarian cancer from the JAVELIN solid tumor phase Ib trial: safety and clinical activity. American Society of Clinical Oncology 2016 Annual Meeting. *J Clin Oncol*. 2016; 34 (suppl; abstr 5533).
- Hassan R, et al. Avelumab (MSB0010718C; anti-PD-L1) in patients with advanced unresectable mesothelioma from the JAVELIN solid tumor phase Ib trial: safety, clinical activity, and PD-L1 expression [abstract]. American Society of Clinical Oncology 2016 Annual Meeting. *J Clin Oncol*. 2016; 34 (suppl) 8503.
- Kelly K, et al. Avelumab (MSB0010718C), an anti-PD-L1 antibody, in patients with metastatic or locally advanced solid tumors: assessment of safety and tolerability in a phase I, open-label expansion study. *J Clin Oncol*. 2015; 33(suppl):abstr 3044.
- Rajan A, et al. Safety and clinical activity of anti-programmed death-ligand 1 (PD-L1) antibody (ab) avelumab (MSB0010718C) in advanced thymic epithelial tumors (TETs). *ASCO Annual Meeting J Clin Oncol*. 2016;34 (suppl; abstr e20106).
- Verschraegen CF, et al. Avelumab (MSB0010718C; anti-PD-L1) as a first-line treatment for patients with advanced NSCLC from the JAVELIN solid tumor phase 1b trial: safety, clinical activity, and PD-L1 expression. American Society of Clinical Oncology 2016 Annual Meeting. *J Clin Oncol*. 2016;34 (suppl; abstr 9036).
- Kaufman HL, et al. Avelumab in patients with chemotherapy-refractory metastatic Merkel cell carcinoma: a multicentre, single-group, open-label, phase 2 trial. *Lancet Oncol*. 2016;17:1374–85.
- LePone LM, et al. Analyses of 123 peripheral human immune cell subsets: defining differences with age and between healthy donors and cancer patients not detected in analysis of standard immune cell types. *J Circ Biomark*. 2016;5. doi:10.05772/62322.
- Madan RA, et al. Effect of talactoferrin alfa on the immune system in adults with non-small cell lung cancer. *Oncologist*. 2013;18:821–2.
- Madan RA, et al. Ipilimumab and a poxviral vaccine targeting prostate-specific antigen in metastatic castration-resistant prostate cancer: a phase 1 dose-escalation trial. *Lancet Oncol*. 2012;13:501–8.
- Ravetch JV, et al. Alternative membrane forms of Fc gamma RIII(CD16) on human natural killer cells and neutrophils. Cell type-specific expression of two genes that differ in single nucleotide substitutions. *J Exp Med*. 1989; 170:481–97.
- Feise RJ. Do multiple outcome measures require p-value adjustment? *BMC Med Res Methodol*. 2002;2:8.
- Wang W, et al. NK cell-mediated antibody-dependent cellular cytotoxicity in cancer immunotherapy. *Front Immunol*. 2015;6:368.
- Huang J, et al. Soluble CD27-pool in humans may contribute to T cell activation and tumor immunity. *J Immunol*. 2013;190:6250–8.
- Huang J, et al. Elevated serum soluble CD40 ligand in cancer patients may play an immunosuppressive role. *Blood*. 2012;120:3030–8.
- Taylor RJ, et al. Fc gamma RIIIa polymorphisms and cetuximab induced cytotoxicity in squamous cell carcinoma of the head and neck. *Cancer Immunol Immunother*. 2009;58:997–1006.
- Conlon KC, et al. Redistribution, hyperproliferation, activation of natural killer cells and CD8 T cells, and cytokine production during first-in-human clinical trial of recombinant human interleukin-15 in patients with cancer. *J Clin Oncol*. 2015;33:74–82.
- Waldmann TA. Interleukin-15 in the treatment of cancer. *Expert Rev Clin Immunol*. 2014;10:1689–701.
- Chen S, et al. A targeted IL-15 fusion protein with potent anti-tumor activity. *Cancer Biol Ther*. 2015;16:1415–21.

27. Dubois S, et al. Preassociation of IL-15 with IL-15R alpha-IgG1-Fc enhances its activity on proliferation of NK and CD8+/CD44high T cells and its antitumor action. *J Immunol*. 2008;180:2099–106.
28. Lehrnbecher T, et al. Variant genotypes of the low-affinity Fcγ receptors in two control populations and a review of low-affinity Fcγ receptor polymorphisms in control and disease populations. *Blood*. 1999;94:4220–32.
29. Farsaci B, et al. Analyses of pretherapy peripheral immunoscore and response to vaccine therapy. *Cancer Immunol Res*. 2016;4:755–65.
30. Czystowska M, et al. The immune signature of CD8(+)/CCR7(+) T cells in the peripheral circulation associates with disease recurrence in patients with HNSCC. *Clin Cancer Res*. 2013;19:889–99.
31. Jordan KR, et al. Myeloid-derived suppressor cells are associated with disease progression and decreased overall survival in advanced-stage melanoma patients. *Cancer Immunol Immunother*. 2013;62:1711–22.
32. Galon J, et al. Type, density, and location of immune cells within human colorectal tumors predict clinical outcome. *Science*. 2006;313:1960–4.
33. Campbell DE, et al. Cryopreservation decreases receptor PD-1 and ligand PD-L1 coinhibitory expression on peripheral blood mononuclear cell-derived T cells and monocytes. *Clin Vaccine Immunol*. 2009;16:1648–53.
34. Binyamin L, et al. Blocking NK Cell Inhibitory Self-Recognition Promotes Antibody-Dependent Cellular Cytotoxicity in a Model of Anti-Lymphoma Therapy. *J Immunol*. 2008;180:6392–401.
35. Voskens CJ, et al. Ex-vivo expanded human NK cells express activating receptors that mediate cytotoxicity of allogeneic and autologous cancer cell lines by direct recognition and antibody directed cellular cytotoxicity. *J Exp Clin Cancer Res*. 2010;29:134.

Submit your next manuscript to BioMed Central and we will help you at every step:

- We accept pre-submission inquiries
- Our selector tool helps you to find the most relevant journal
- We provide round the clock customer support
- Convenient online submission
- Thorough peer review
- Inclusion in PubMed and all major indexing services
- Maximum visibility for your research

Submit your manuscript at
www.biomedcentral.com/submit

